M&C 2017 - International Conference on Mathematics & Computational Methods Applied to Nuclear Science & Engineering, Jeju, Korea, April 16-20, 2017, on USB (2017)

Kriging-based Surrogate Models for Uncertainty Quantification and Sensitivity Analysis

Xu Wu, Chen Wang, Tomasz Kozlowski

Department of Nuclear, Plasma and Radiological Engineering
University of Illinois at Urbana-Champaign
224 Talbot Laboratory, 104 South Wright Street, Urbana, Illinois, 61801, USA
xuwu2@illinois.edu, chenw3@illinois.edu, txk@illinois.edu

Abstract - *In this paper, we propose to use Kriging (also called Gaussian Process emulators) surrogate models for uncertainty and sensitivty analysis in nuclear engineering. The motivation is to significantly reduce the computational cost while maintaining a desirable accuracy. Kriging modeling only requires the input/output relations of the full model and thus can treat the full model as a black box. We investigated the Point Reactor Kinetics Equation (PRKE) with lumped parameter thermal-hydraulics feedback model to compare Monte Carlo (MC) sampling, Polynomial Chaos Expansion (PCE) and Kriging surrogate model for uncertainty and sensitivity analysis. We applied Principal Component Analysis (PCA) for the dimension reduction. The Kriging surrogate models are built for the principal component scores. Comparison of the statistical moments of results from MC sampling of the full model, PCE and Kriging surroagte model shows that the Kriging surrogate model can accurately predict the statistical moments of the full model outputs. It only requires tens to a few hundreds of full model runs for the training and after that it can be executed with negligible cost.*

I. INTRODUCTION

Within the BEPU (Best Estimate plus Uncertainty) [1] methodology uncertainties must be quantified in order to prove that the investigated design remains within acceptance criteria. This requires the propagation of input uncertainties to the output predictions, known as Uncertainty Quantification (UQ). Sensitivity analysis (SA) is the study of how uncertain input parameters contribute to the variation in the output. Reliable UQ and SA are significant parts of modelling and simulation.

Modern nuclear system simulations emphasize improvements of computational accuracy. One of the main directions to achieve this is to use coupled multi-physics approach with high fidelity simulators. The term “multi-physics” means the requirement of coupling of discrete physics. Coupled systems that integrate relevant phenomena in reactor systems such as neutronics, thermal-hydraulics, and fuel performance analysis are needed to improve design, operation and safety methodologies of modern reactors.

Extensive UQ and SA efforts are subsequently required for such multi-physics coupled simulations, which poses challenges to the current UQ and SA methodologies as listed below:

1. The nuclear reactor physics simulation normally involves high dimensionality spaces (e. g. cross-sections), while thermal-hydraulics and fuel performance modeling commonly includes strong non-linear phenomena.
2. Perturbation theory and adjoint approaches are less suitable when large uncertainty and non-linear effects are significant.
3. Stochastic spectral methods like Polymial Choas Expansion and Stochastic Collocation are very efficient and can have spectral convergence if well-designed, but their performance is greatly limited from the notorious "Curse of Dimensionality".
4. Brute force Monte Carlo (MC) sampling is robust and independent of the model dimension. But it has extremely slow convergence rate and requires large number of simulations, which is impractical for many simulation codes in nuclear engineering even with high performance computing.

In this paper, we propose to use Kriging-based surrogate models [2] [3] [4] [5] for UQ and SA in nuclear engineering. Surrogate model is an approximation of the input/output relation of a compututer code/model. It is also called metamodel, response surface or emulator. Surroagte models usually take much less computational time than the full model (like TRACE, BISON, etc.) while maintaining the input/output relation of the original model to a desirable accuracy. Constructing the surrogate models normally requires small number of executions of the original model. Once validated, surrogate models can be used to perform uncertainty and sensitivity analysis, Bayesian inversion, optimization, etc.

II. THEORY

1. Essential Components of Kriging

In statistics, Gaussian process regression [6] [7] is widely used as a method of interpolation for which the interpolated values are modeled by a Gaussian process. In geostatistics (also known as spatial statistics), regression with Gaussian processes is known as Kriging [3]. Kriging has been widely used as surrogate models for deterministic computer models. A Kriging model is a generalized linear regression model that accounts for the correlation in the residuals between the regression model and the observations.

Consider a computer model $y = G(\mathbf{x})$. Without loss of generality, consider y as a scalar and $\mathbf{x}$ is a d-dimensional vector representing d input parameters. Assuming that the computer model output is known at m design sites $\mathbf{X} = (\mathbf{x}_1, \mathbf{x}_2, \ldots, \mathbf{x}_m)^\top$. The corresponding output values are $\mathbf{y} = (y_1, y_2, \ldots, y_m)^\top =$

$[G(\mathbf{x}_1), G(\mathbf{x}_2), \ldots, G(\mathbf{x}_m)]^\top$.

The mathematical form of a Kriging model has two parts:

$$\hat{y}(\mathbf{x}) = \sum_{j=1}^{n} \beta_j f_j(\mathbf{x}) + z(\mathbf{x}) = \mathbf{f}^\top(\mathbf{x})\boldsymbol{\beta} + z(\mathbf{x}) \tag{1}$$

where $\mathbf{f} = [f_1, f_2, \ldots, f_n]^\top$. The first part is a linear regression of the data with n regressors modeling the drift of the process mean. The second part $z(\mathbf{x})$ is a stationary Gaussian random process with zero mean and covariance:

$$\mathrm{Cov}\left[z(\mathbf{x}_i), z(\mathbf{x}_j)\right] = \sigma^2 \mathcal{R}\left(\mathbf{x}_i, \mathbf{x}_j\right) \tag{2}$$

where σ^2 is the process variance.

The spatial correlation function (SCF) $\mathcal{R}\left(\mathbf{x}_i, \mathbf{x}_j\right)$ controls the smoothness of the resulting Kriging model and the influence of nearby points. The Gaussian function is the most commonly used SCF as it provides a relatively smooth and infinitely differentiable surface:

$$\mathcal{R}\left(\mathbf{x}_i, \mathbf{x}_j\right) = \mathcal{R}\left(|\mathbf{x}_i - \mathbf{x}_j|\right) = e^{-\frac{|\mathbf{x}_i - \mathbf{x}_j|^2}{\theta}} \tag{3}$$

TABLE I: Common spatial correlation functions (or correlation kernels)

Name	Expression $\left(h = \lvert\mathbf{x}_i - \mathbf{x}_j\rvert\right)$
Exponential	$\mathcal{R}(h) = \exp\left(-\frac{\lvert h\rvert}{\theta}\right)$
Power-exponential	$\mathcal{R}(h) = \exp\left(-\frac{\lvert h\rvert^p}{\theta^p}\right)$
Gaussian	$\mathcal{R}(h) = \exp\left(-\frac{\lvert h\rvert^2}{2\theta^2}\right)$
Matern $\nu = 3/2$	$\mathcal{R}(h) = \left(1 + \frac{\sqrt{3}\lvert h\rvert}{\theta}\right)\exp\left(-\frac{\sqrt{3}\lvert h\rvert}{\theta}\right)$
Matern $\nu = 5/2$	$\mathcal{R}(h) = \left(1 + \frac{\sqrt{5}\lvert h\rvert}{\theta} + \frac{5h^2}{3\theta^2}\right)\exp\left(-\frac{\sqrt{5}\lvert h\rvert}{\theta}\right)$

The correlation function scale parameter θ is essentially a width parameter which affects how far a sample point's influence extends. Different θ's can be chosen for different input dimensions:

$$\mathcal{R}\left(|\mathbf{x}_i - \mathbf{x}_j|\right) = \prod_{k=1}^{d} e^{-\frac{|x_{i,k} - x_{j,k}|^2}{\theta_k}} \tag{4}$$

2. Prediction using Kriging Surrogate Model

Given the design sites $\mathbf{X}$ and corresponding output values $\mathbf{Y}$, to predict the output values at a new input location $\mathbf{x}^*$ using the Kriging model, we first define the following notations:

1. The set of regression functions $\mathbf{f} = [f_1, f_2, \ldots, f_n]^\top$ evaluated at the unknown point $\mathbf{x}^*$:

$$\mathbf{f}(\mathbf{x}^*) = \left[f_1(\mathbf{x}^*), f_2(\mathbf{x}^*), \ldots, f_n(\mathbf{x}^*)\right]^\top$$

2. The set of regression functions evaluated at m known design points:

$$\mathbf{F} = [\mathbf{f}(\mathbf{x}_1), \mathbf{f}(\mathbf{x}_2), \ldots, \mathbf{f}(\mathbf{x}_m)]^\top = \begin{bmatrix} f_1(\mathbf{x}_1) & f_2(\mathbf{x}_1) & \cdots & f_n(\mathbf{x}_1) \\ f_1(\mathbf{x}_2) & f_2(\mathbf{x}_2) & \cdots & f_n(\mathbf{x}_2) \\ \vdots & \vdots & \ddots & \vdots \\ f_1(\mathbf{x}_m) & f_2(\mathbf{x}_m) & \cdots & f_n(\mathbf{x}_m) \end{bmatrix}$$

3. The correlation of $\mathbf{x}^*$ with design points $\mathbf{X}$:

$$\mathbf{r}(\mathbf{x}^*) = \left[\mathcal{R}(\mathbf{x}^*, \mathbf{x}_1), \mathcal{R}(\mathbf{x}^*, \mathbf{x}_2), \ldots, \mathcal{R}(\mathbf{x}^*, \mathbf{x}_m)\right]^\top$$

4. The correlation matrix $\mathbf{R}$ of design points $\mathbf{X}$:

$$\mathbf{R} = \begin{bmatrix} \mathcal{R}(\mathbf{x}_1, \mathbf{x}_1) & \mathcal{R}(\mathbf{x}_1, \mathbf{x}_2) & \cdots & \mathcal{R}(\mathbf{x}_1, \mathbf{x}_m) \\ \mathcal{R}(\mathbf{x}_2, \mathbf{x}_1) & \mathcal{R}(\mathbf{x}_2, \mathbf{x}_2) & \cdots & \mathcal{R}(\mathbf{x}_2, \mathbf{x}_m) \\ \vdots & \vdots & \ddots & \vdots \\ \mathcal{R}(\mathbf{x}_m, \mathbf{x}_1) & \mathcal{R}(\mathbf{x}_m, \mathbf{x}_2) & \cdots & \mathcal{R}(\mathbf{x}_m, \mathbf{x}_m) \end{bmatrix}$$

Then, the best linear unbiased predictor (BLUP) of $\hat{y}(\mathbf{x}^*)$ is:

$$\hat{y}(\mathbf{x}^*) = \mathbf{f}^\top(\mathbf{x}^*)\hat{\boldsymbol{\beta}} + \mathbf{r}^\top(\mathbf{x}^*)\mathbf{R}^{-1}\left(\mathbf{y} - \mathbf{F}\hat{\boldsymbol{\beta}}\right) \tag{5}$$

where $\hat{\boldsymbol{\beta}}$ is the least sqaures estimate of $\boldsymbol{\beta}$:

$$\hat{\boldsymbol{\beta}} = \left(\mathbf{F}^\top\mathbf{R}^{-1}\mathbf{F}\right)^{-1}\mathbf{F}^\top\mathbf{R}^{-1}\mathbf{y} \tag{6}$$

The MSE or variance of the estimate $\hat{y}(\mathbf{x}^*)$ is:

$$\mathrm{MSE}\left[\hat{y}(\mathbf{x}^*)\right] = \sigma^2\left\{1 - \mathbf{r}^\top(\mathbf{x}^*)\mathbf{R}^{-1}\mathbf{r}(\mathbf{x}^*) + \left(\mathbf{r}^\top(\mathbf{x}^*)\mathbf{R}^{-1}\mathbf{F} - \mathbf{f}^\top(\mathbf{x}^*)\right)^\top\left(\mathbf{F}^\top\mathbf{R}^{-1}\mathbf{F}\right)^{-1}\left(\mathbf{r}^\top(\mathbf{x}^*)\mathbf{R}^{-1}\mathbf{F} - \mathbf{f}^\top(\mathbf{x}^*)\right)\right\} \tag{7}$$

Equations 5 to 7 formulate the so called Universal Kriging (UK). Ordinary Kriging (OK) is a special case of UK when the basis functions reduce to a unique constant function, $\mathbf{f}(\mathbf{x}) = [1]$. Simple Kriging (SK) is the case when the mean function is a known deterministic function:

$$\hat{y}(\mathbf{x}) = \mu(\mathbf{X}) + \mathbf{r}^\top(\mathbf{x})\mathbf{R}^{-1}\left(\mathbf{y} - \mu(\mathbf{X})\right) \tag{8}$$

$$\mathrm{MSE}\left[\hat{y}(\mathbf{x})\right] = \sigma^2\left\{1 - \mathbf{r}^\top(\mathbf{x})\mathbf{R}^{-1}\mathbf{r}(\mathbf{x})\right\} \tag{9}$$

The Kriging model can be proved to be **interpolating** all the design points. The predicted variance increases as new point gets further away from existing points. To build Kriging surrogate model, we only need to run the original model $y = G(\mathbf{x})$ m times, which depends on the desired accuracy level (m is typically a few hundreds). Once the Kriging surrogate model is available, we can use it for prediction at new point $\mathbf{x}^*$, which will run practically instantaneously.

III. SIMULATION MODEL

To test the proposed methodology, the Point Reactor Kinetics Equation (PRKE) with lumped parameter thermal-hydraulics feedback model [8] [9] will be used in this study. It describes the transient behavior of the normalized power level $p(t)$, the delayed neutron precursor concentrations $C(t)$, and the core effective fuel and coolant temperatures, $T_{\mathrm{fuel}}(t)$ and $T_{\mathrm{cool}}(t)$. The model employs the standard neutron point kinetic equations and couples them to simple 0-D (core average) fuel heat conduction and fluid energy balance models via the reactivity function. In this model, the reactivity depends

TABLE II: Symbols used in Kriging formulation

Symbol	Dimension	Description
d	1×1	number of input factors
m	1×1	number of design points
n	1×1	number of basis functions
$\boldsymbol{\beta}$	$n \times 1$	vector of regression coefficients
$\hat{\boldsymbol{\beta}}$	$n \times 1$	estimate of $\boldsymbol{\beta}$
$\mathbf{f}$	$n \times 1$	vector of regression functions $\mathbf{f} = [f_1, f_2, \ldots, f_n]^\top$
$\mathbf{x}_i$	$d \times 1$	vector of i^{th} design point, $\mathbf{x}_i = \left(x_{i,1}, x_{i,2}, \ldots, x_{i,p}\right)^\top$
y_i	1×1	output value of i^{th} design point, $y_i = G(\mathbf{x}_i)$
$\mathbf{X}$	$m \times d$	collection of m design points
$\mathbf{y}$	$m \times 1$	vector of output values at $\mathbf{X}$, $\mathbf{y} = (y_1, y_2, \ldots, y_m)^\top$
$\mathbf{x}^*$	$d \times 1$	unknown input point, to be predicted
$\hat{y}(\mathbf{x}^*)$	1×1	predicted output at $\mathbf{x}^*$
$\mathbf{f}(\mathbf{x}^*)$	$n \times 1$	$\mathbf{f}$ evaluated at $\mathbf{x}^*$
$\mathbf{F}$	$m \times n$	$\mathbf{f}$ evaluated at $\mathbf{X}$
$\mathbf{r}(\mathbf{x}^*)$	$m \times 1$	correlation between $\mathbf{x}^*$ and design points $\mathbf{X}$
$\mathbf{R}$	$m \times m$	correlation between design points $\mathbf{X}$

on both fuel and coolant temperatures. The system of coupled nonlinear Ordinary Differential Equations (ODEs) is given by:

$$\frac{dp(t)}{dt} = \frac{\rho(t, T_{\text{fuel}}, T_{\text{cool}}) - \beta}{\Lambda} p(t) + \lambda C(t) \tag{10}$$

$$\frac{dC(t)}{dt} = \frac{\beta}{\Lambda} p(t) - \lambda C(t) \tag{11}$$

$$\frac{dT_{\text{fuel}}(t)}{dt} = \frac{\Omega_{\text{pow}} p(t)}{\rho_{\text{fuel}} c_{\text{p, fuel}}} - \frac{[T_{\text{fuel}}(t) - T_{\text{cool}}(t)]}{\rho_{\text{fuel}} c_{\text{p, fuel}} \hat{R}_{th}} \tag{12}$$

$$\frac{dT_{\text{cool}}(t)}{dt} = -\frac{2u}{H}\left[T_{\text{cool}} - T_{\text{cool}}^{in}\right] + \frac{A_{\text{fuel}}}{A_{\text{flow}}} \frac{[T_{\text{fuel}}(t) - T_{\text{cool}}(t)]}{\rho_{\text{cool}} c_{\text{p, cool}} \hat{R}_{th}} \tag{13}$$

Note that only one-group effective delayed neutron is considered. The detailed definitions of the parameters and values used in the model can be found in [9]. The fuel and cladding material properties are based on LWR fuel and cladding properties [10] [11]. The lumped parameter (i.e. averaging the unknown values over the whole domain) description of the reactor fuel and coolant temperatures allows the elimination of the spatial dependencies and therefore focuses on the time-dependent part.

In this model, the neutronics equations (the first two equations) are coupled to the thermal-hydraulics equations (the last two equations) via the temperature dependent total reactivity $\rho(t, T_{\text{fuel}}, T_{\text{cool}})$ that contains the external reactivity term (e.g., control rod movement), the fuel temperature reactivity and the coolant temperature reactivity:

$$\rho(t, T_{\text{fuel}}, T_{\text{cool}}) = \rho_{\text{ext}} - \alpha_D[T_{\text{fuel}}(t) - T_{\text{fuel}}(0)] - \alpha_c[T_{\text{cool}}(t) - T_{\text{cool}}(0)] \tag{14}$$

In the above equation, ρ_{ext}, α_D and α_c are external reactivity insertion, Doppler reactivity coefficient and coolant temperature coefficient, respectively. These three parameters are treated as uncertain input parameters in the model. The Quantity of Interests (QoIs) in this model are $p(t)$, $C(t)$, $T_{\text{fuel}}(t)$ and $T_{\text{cool}}(t)$.

TABLE III: Uncertainties for three input parameters

Parameters	mean	std/mean
ρ_{ext}	$0.8 \cdot \rho_{\text{ext},0}$	20%
α_D	$1.5 \cdot \alpha_{D,0}$	20%
α_c	$1.5 \cdot \alpha_{c,0}$	20%

We arbitrarily chose some uncertainties for the input parameters as shown in Table III, as the main purpose is to compare MC sampling, PCE and Kriging-based surrogate model for uncertainty and sensitivty analysis. In Table III, $\rho_{\text{ext},0} = \beta$, $\alpha_{D,0} = 3.18 \times 10^{-3}\beta$, $\alpha_{c,0} = 8.2186 \times 10^{-3}\beta$ are nominal values used in [8]. Figure 1 shows the Probability Density Functions (PDFs) of the three uncertain input parameters.

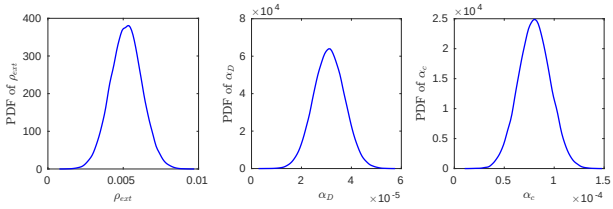

Fig. 1: PDFs for three random input parameters

The reasons of choosing this model for testing the Kriging surrogate modeling are listed below:

1. This model is essentially a mini-multiphysics problem, which has been designed as close to a real reactor as possiblel. All the material properties are based on Westinghouse PWR [9].

2. It takes very short simulation time to run (about 0.5 sec-

onds), which makes MC sampling available as a reference solution.

3. Solutions from PCE [9] are available for comparison. Intrusive Galerkin projection can be directly applied to this model since we know the exact form of the ODEs.

4. This model involves multiple (three) uncertainty input parameters, as well as multiple (four) QoIs.

5. The four QoIs are time-dependent, which is a challenging topic for surrogate modeling. Normally Principal Component Analysis (PCA) is required for data reduction.

IV. RESULTS AND ANALYSIS

1. Simulation at Nominal Input Values and Input Uncertainties

This model starts from an initial condition of $p(t = 0) = 1.0$, while initial conditions for $C(t)$, $T_{\text{fuel}}(t)$ and $T_{\text{cool}}(t)$ can be found in [9]. Figures 2 and Figure 3 show the simulation results at mean values of the three uncertain input parameters. With the introduction of external reactivity, the power quickly increases to about four times of the initial state. Consequently, the fuel and coolant temperature increase introduces negative feedback to counter-interact the external reactivity, and the power returns to a new lower value in a short time.

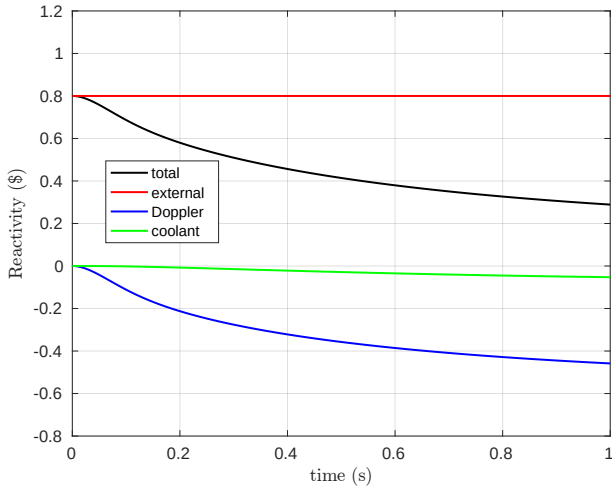

Fig. 2: Reactivity evolution at nominal values of the random uncertain input parameters

The increase in coolant temperature is small and the negative reactivity feedback caused by the coolant is negligible, which will cause the system to be insensitive to coolant temperature coefficient α_c.

2. UQ Solution using Monte Carlo Sampling and Polynomial Choas Expansion

To provide reference solutions for Kriging-based surrogate models, we performed the MC sampling (with 5000 samples) and PCE with intrusive Galerkin approach up to polynomial order 5. Details of the PCE derivation and implementation can be found in [9]. In this paper we only provide the results.

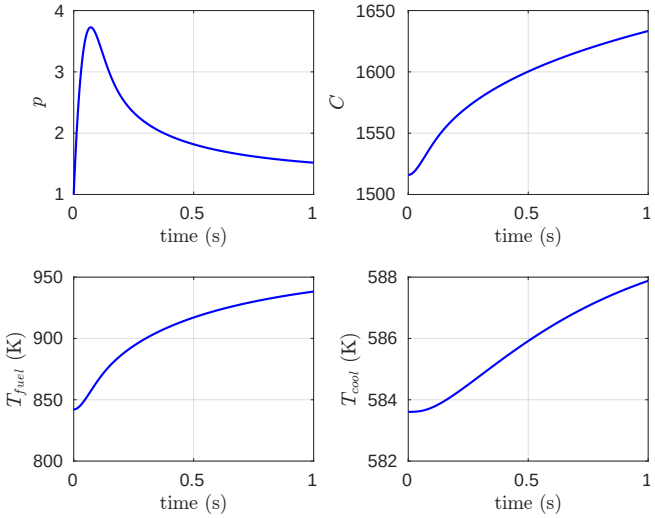

Fig. 3: Simulation results for the four QoIs at nominal values of the random input parameters

Figure 4 shows the comparison of the mean values for four QoIs predicted by the MC sampling and PCE with order up to 5. Here we only compare results at 21 time points which are uniformly distributed between 0 and 1 second. There is an excellent agreement of these results. PCE can accurately predict the mean values even at a very low expansion order.

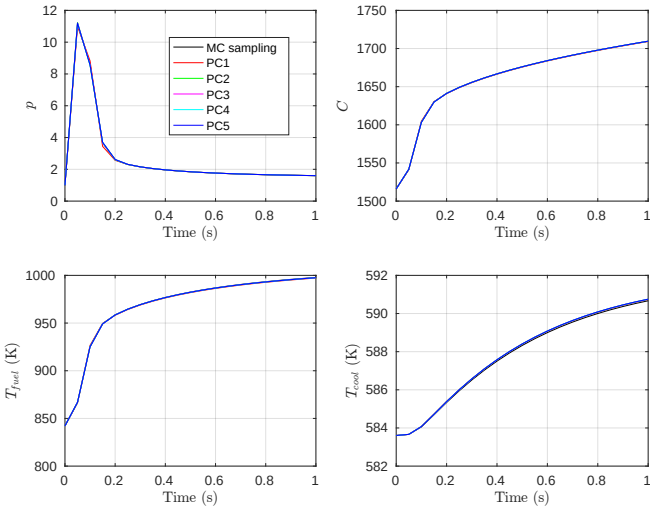

Fig. 4: Mean values of four QoIs by MC sampling and PCE

Figure 5 shows the comparison of the standard deviations for four QoIs predicted by the MC sampling and PCE with order up to 5 for different priors. For p (normalized power) and C (delay neutron precursors) the PCE predicted standard deviations converge to the MC sampling values, while for T_{fuel} and T_{cool} PCE predictions converge to values that are slightly different than MC sampling standard deviations. They are likely to be caused by the PCE low order truncation in both inputs and outputs. The ODEs for T_{fuel} and T_{cool} include many material properties that depend on T_{fuel} and T_{cool} themselves,

causing them to be more sensitive to small errors than p and C, which are only affected by T_{fuel} and T_{cool}. However, these discrepancies are very small compared to the mean values of those QoIs.

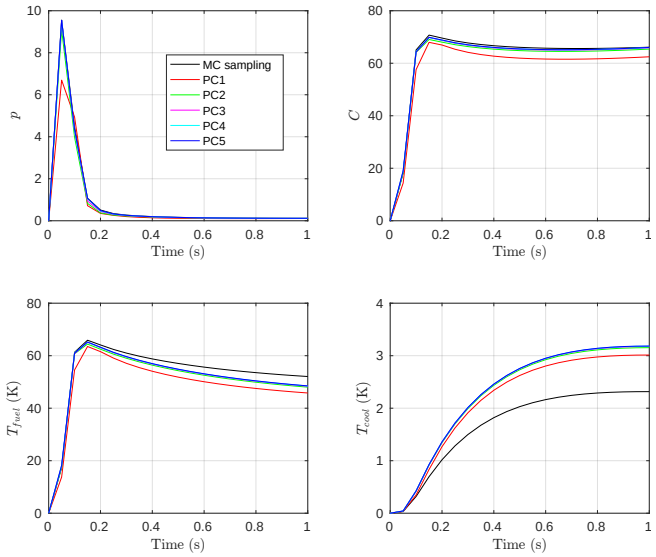

Fig. 5: Standard deviations of four QoIs by MC sampling and PCE

3. Principal Component Analysis for Dimension Reduction

The remaining issue before building surrogate models by Kriging is that the four QoIs are time-dependent, which causes each QoI to be multivariate. If we are interested in many time steps of these four QoIs, the dimension of the outputs can be very high. It is not efficient to build surrogate models for each QoI at each time step. So we used PCA as a dimension reduction technique to reduce the number of outputs. In the following, we will use T_{fuel} as an example to demonstrate this process.

Suppose now we are interested in $p = 21$ time points in the T_{fuel} evolution. These p time points are uniformly distributed between 0 and 1 second. The intuition for dimension reduction is that by observing the evolution of T_{fuel} shown in Figure 3, we noticed that the shape is nearly linear or close to a quadratic polynomial. We do not need so many ($p = 21$) "variables" to represent such a shape. To learn the underlying pattern of the evolution of T_{fuel}, we sample the input parameters N times, run the model and collect the T_{fuel} data and center the data to form a $p \times N$ data matrix $\mathbf{A}$.

Define the following linear transformation:

$$\mathbf{PA} = \mathbf{B} \tag{15}$$

where $\mathbf{P}$ is a $p \times p$ transformation matrix and $\mathbf{B}$ is a $p \times N$ data martrix whose rows represented new variables.

Now the covariance matrix of $\mathbf{A}$ is a full matrix. After the transformation, we would like matrix $\mathbf{B}$ to have a diagonal covariance matrix, which means that the new variables in $\mathbf{B}$ are independent. To find such a transformation matrix $\mathbf{P}$, we first look at the Singular Value Decomposition (SVD) of $\mathbf{A}$:

$$\mathbf{A} = \mathbf{U}\mathbf{\Sigma}\mathbf{V}^\top \tag{16}$$

where

1. $\mathbf{U}$ is a $p \times p$ orthogonal matrix. The columns of $\mathbf{U}$ are called the **left-singular vectors** of $\mathbf{A}$. The columns of $\mathbf{U}$ are a set of orthonormal eigenvectors of $\mathbf{A}\mathbf{A}^\top$.

2. $\mathbf{V}$ is a $N \times N$ orthogonal matrix. The columns of $\mathbf{V}$ are called the **right-singular vectors** of $\mathbf{A}$. The columns of $\mathbf{V}$ are a set of orthonormal eigenvectors of $\mathbf{A}^\top\mathbf{A}$.

3. $\mathbf{\Sigma}$ is a $p \times N$ rectangular diagonal matrix with non-negative real numbers on the diagonal. The diagonal entries σ_i of $\mathbf{\Sigma}$ are called the **singular values** of $\mathbf{A}$ and are arranged in descending order. Singular values are square roots of the eigenvalues of $\mathbf{A}\mathbf{A}^\top$ and $\mathbf{A}^\top\mathbf{A}$. Large singular values point to important features in matrix $\mathbf{A}$.

If we choose $\mathbf{P} = \mathbf{U}^\top$, we have:

$$\mathbf{PA} = \mathbf{U}^\top\mathbf{A} = \mathbf{\Sigma}\mathbf{V}^\top = \mathbf{B} \tag{17}$$

$$\mathbf{C_B} = \text{Cov}(\mathbf{\Sigma}\mathbf{V}^\top) = \frac{1}{N}\mathbf{\Sigma}\mathbf{V}^\top\mathbf{V}\mathbf{\Sigma} = \frac{1}{N}\mathbf{\Sigma}^2 \tag{18}$$

It can be seen that if we choose $\mathbf{P} = \mathbf{U}^\top$, whose columns are the left-singular vectors of $\mathbf{A}$, the covariance matrix of $\mathbf{Y}$ is diagonalized. Define the following:

1. The rows of $\mathbf{P}$ are called **principal components**, also known as loadings. Each row of $\mathbf{P}$ contains coefficients for one principal component (a vector of length p).

2. The transformed variables (rows of $\mathbf{B}$) are called **principal component scores**. Principal component scores are the representations of the original data $\mathbf{A}$ in the principal component space. The columns of $\mathbf{B}$ correspond to observations.

3. The eigenvalues of the covariance matrix of $\mathbf{A}$ are called **principal component variances**, which correspond to the sqaure of the diagonal elements in $\mathbf{\Sigma}$.

Note that diagonal entries of $\mathbf{\Sigma}$ are arranged in decending order. It is quite normal that the values of such entries decrease very quickly. We can remove the entries that has very small values, which corresponds to only keeping the first few principal components. Suppose we only keep the first p^* principal components:

$$\mathbf{P}^*\mathbf{A} = \mathbf{B}^* \tag{19}$$

where $\mathbf{P}$ is a $p^* \times p$ transformation matrix and $\mathbf{B}$ is a $p^* \times N$ data martrix whos rows represented new variables after reduction. Now we have reduced the the number of variables from p to p^*. A commonly accepted criteria is that the reserved variables have variances that account for over 95% (some others choose 99%) of the total variance.

To find the principal components in the current study, we run the model with $N = 25, 50, 100, 200$ samples. Figure 6

shows the decay of the principal component variances. Clearly, the variances become trivial after first few dimensions.

Figure 7 shows the percentage of total variance explained by each dimension. Figure 8 shows the cumulative percentage of total variance explained. Clearly the first two variables can account for over 99.8% percent of the total variation, which means that we only need the first **two** principal components. Therefore, the dimension of the output T_{fuel} has been reduced from 21 to 2 and in the following we only need to build Kriging surrogate models for these two new variables.

Figure 9 shows the first two (p^*) principal components (each one is a p-vector). The first principal component is similar in shape with the evolution of T_{fuel} and it dominates the change of T_{fuel} with time. The second principal component represents the influence of power p on T_{fuel}. T_{fuel} first increases because of the power surge. Then thn increasing rate becomes smaller because of the negative weighting from the second principal component.

4. Build and Validate the Kriging Surrogate Model

In the last section we have found the principal components for T_{fuel} and performed the dimension reduction. In this section we will build the Kriging surrogate models follow the steps below:

1. Create the N training samples by Latin Hypercube Sampling (LHS) [12].
2. Run the PRKE model at the training samples, get the $p \times N$ data matrix $\mathbf{A}$. Calculate the mean and center this data matrix by substracting the mean.
3. Perform PCA of the centered data matrix. Find the first p^* principal components which forms a $p^* \times p$ matrix $\mathbf{P}^*$, and the corresponding principal component scores. Note that each score will have N samples.
4. Build Kriging surrogate model for each principal component score based on the N samples.
5. Use the Kriging surrogate model to make prediction. At every new sample of the inputs, the Kriging model produce prediction for each score which forms a $p^* \times 1$ vector $\mathbf{b}$.
6. With $\mathbf{a} = \mathbf{P}^{*\top}\mathbf{b}$ we can get a $p \times 1$ vector $\mathbf{a}$, which represents the time evolution T_{fuel} after adding the mean vector back.

As we have a few options for correlations kernels and many choices for the trend functions, we need to find the most appropriate combinations for the following study. This can be done by a simple test to see if the Kriging model can reproduce the T_{fuel} results at mean values of the uncertain inputs. Figure 10 shows the predictions of Kriging surrogate models built using different kind of correlation kernels and same training samples ($N = 100$) and trend functions (constant). The first three subfigures show the predictions along with the standard deviations of the prediction. And the last subfigure shows the comparison of T_{fuel} from various Kriging predictions with results from running the full model. Even though all the Kriging

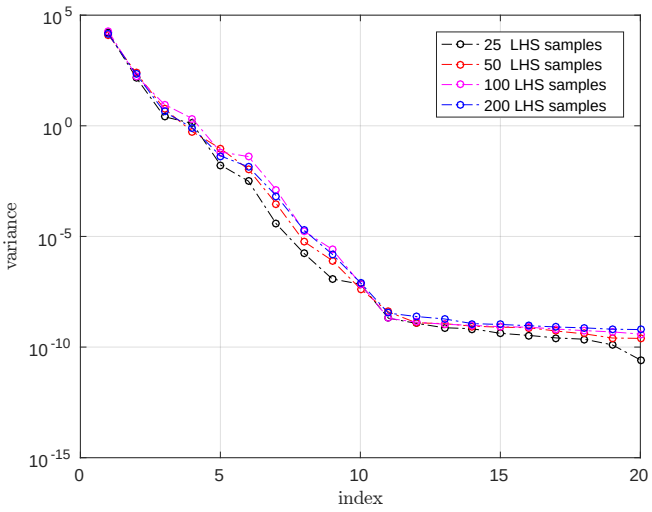

Fig. 6: Decay of principal component variances

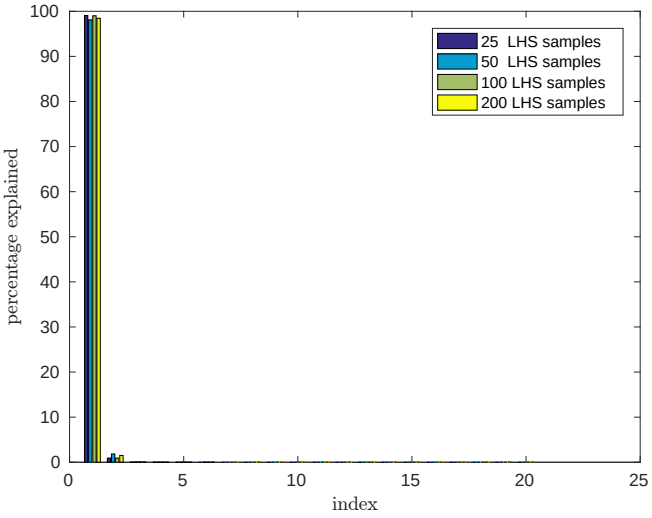

Fig. 7: Percentage of total variation explained

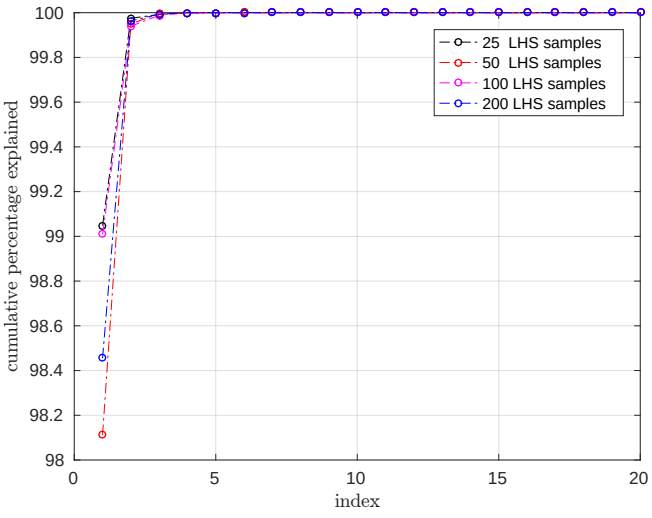

Fig. 8: Cumulative percentage of total variation explained

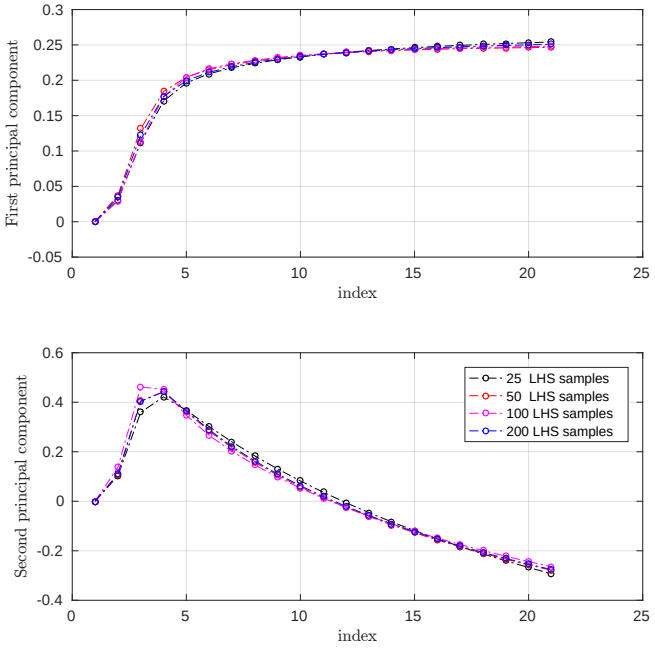

Fig. 9: First and second principal components

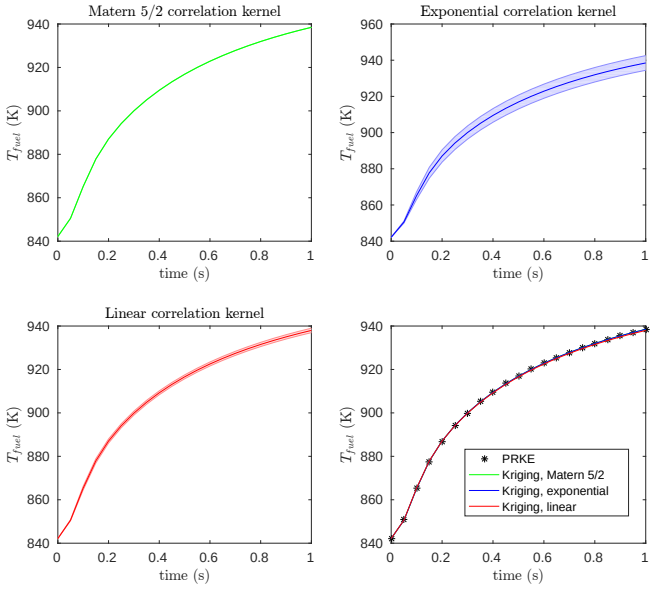

Fig. 10: Comparison of T_{fuel} from PRKE and Kriging surrogate models with different correlation kernels

mdoels can accurately reproduce the T_{fuel} evolution, the Kriging models built with linear and exponential correlation kernel have large variances in their predictions. In the following we will choose the Matern 5/2 correlation kernel.

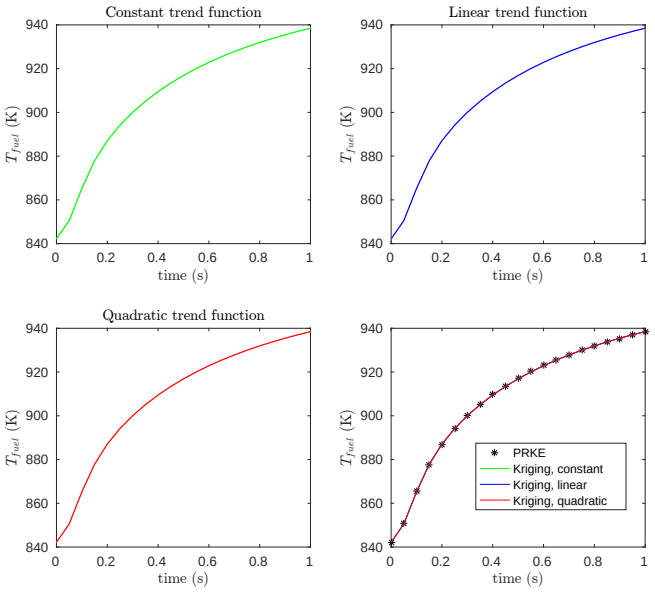

Fig. 11: Comparison of T_{fuel} from PRKE and Kriging surrogate models with different trend functions

Figure 11 shows comparison for different trend functions: constant, linear and quadratic. No obvious difference can be observed for different cases. Actually Ordinary Kriging (with constant trend functions) is the most widely used version of Kriging surrogate model. In the following we will choose the constant trend function.

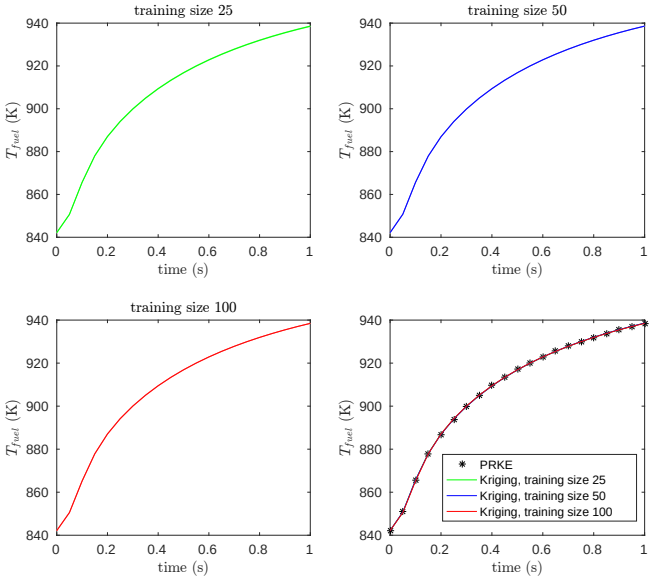

Fig. 12: Comparison of T_{fuel} from PRKE and Kriging surrogate models with different number of training samples

Figure 12 shows the comparison for different sample sizes. We can see that even with a small training sample size ($N = 25$)

the Kriging predictions are very accurate. To better evaluate the performance of Kriging model with training sample sizes $N = 25, 50, 100$, we can use the sample set with size 200 for validation (we can also use Cross Validation). The validation is performed based on the accuracy of the Surrogate model's capability to predict the responses at samples other than the training sites. The predictivity coefficient Q_2 is usually used to evaluate the fitted Kriging surrogate model:

$$Q_2 = 1 - \frac{\sum_{i=1}^{N_{\text{val}}} \left(Y_i - \hat{Y}_i\right)}{\sum_{i=1}^{N_{\text{val}}} \left(\bar{Y} - Y_i\right)} \tag{20}$$

where N_{val} is the size of the validation set (in this case 200). Y_i denotes full model simulation outputs of the validation set and $\bar{Y}$ is their empirical mean. $\hat{Y}_i$ represents the prediction from Kriging surrogate model. In practical situations, a metamodel with a predictivity oefficient above than 0.7 is often considered as a satisfactory approximation of the computer code [13]. Table IV shows the predictivity coefficients for both principal component scores and all the training samples. The predictivity coefficient is above 97.5% even with a samll number of training samples ($N = 25$).

TABLE IV: Predictivity coefficients Q_2

Training sample size	score 1	score 2
25	0.9984	0.9753
50	0.9988	0.9975
100	0.9995	0.9988

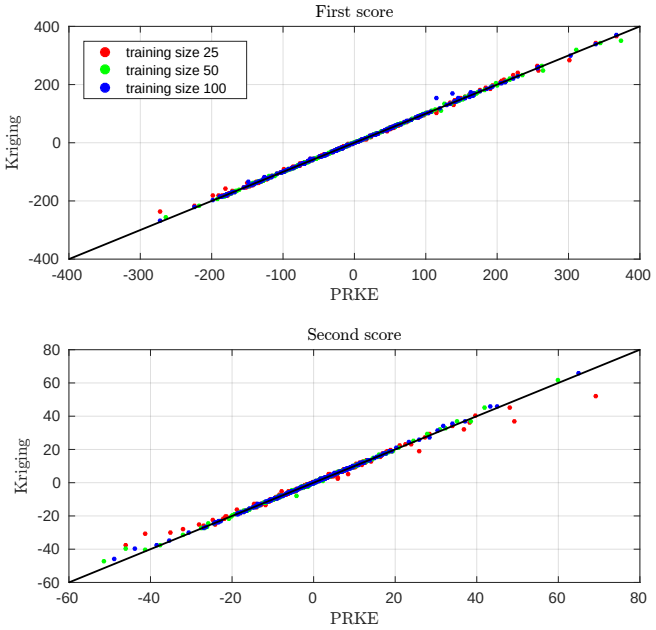

Fig. 13: Comparison of first and second PCA scores from PRKE and Kriging surrogate models with different training sizes.

Figure 13 shows the comparison of first and second PCA scores from PRKE and Kriging surrogate models with different training sizes. It is observed that most of the points fall very close to the diagonal line, with only a few exceptions for $N = 25$.

The primary assumption of Kriging surrogate model is that the response of the computer model under consideration is a sample path of an underlying Gaussian random field. It indicates that the output responses at different samples follow joint Gaussian distributions. Kriging surrogate model can not only provide the response prediction, but also the Mean Squared Error (MSE, or variance) of its prediction. The differences between full model simulations and Kriging metamodel predictions are called residuals. And by dividing the residuals by the corresponding standard deviations of the prediction we get the standardized residuals. By assumption the standardized residuals follow the standard normal distribution. Therefore, 99.7% of all the standardized residuals are expected to fall within $[-3, 3]$. This is also verified by Figure 14. As expected, the case with $N = 25$ has the most points that fall above 3 or below -3. In the following we will use the training sample set of size 50 to build the Kriging surrogate model for uncertainty and sensitivity analysis.

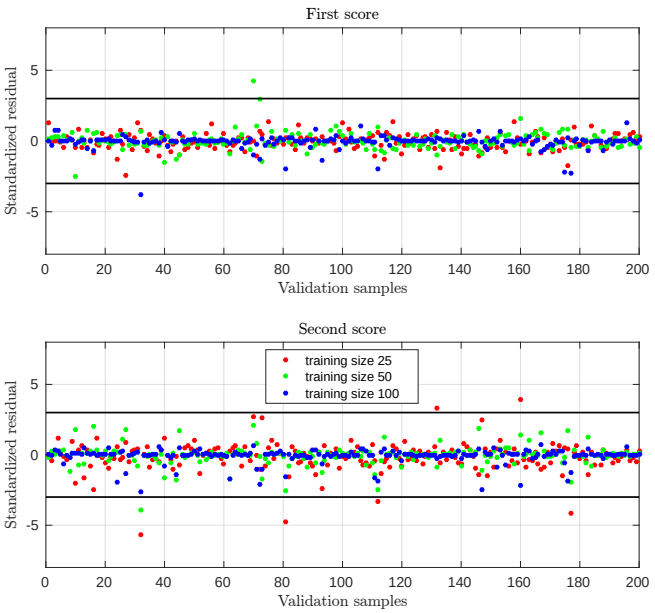

Fig. 14: Standardized residuals for first and second PCA scores from Kriging surrogate models with different training sizes.

5. Uncertainty and Sensitivity Analysis using Kriging Surrogate Model

In the last section we have selected Matern 5/2 correlation kernel, constant trend function and training samples of size 50 to build the Kriging surrogate model and successfully validated the surrogate model. Now we can use Kriging model for uncertainty and sensitivity anlaysis by sampling it at arbitrary input locations. The advantage and primary purpose of using Kriging surrogate model is that it can be evaluated in a negligible time. For example. 10,000 evaluations of the current Kriging model only take about 19 seconds using a single processor.

Figure 15 and 16 show the comparison of mean values and standard deviations of T_{fuel} w.r.t. time, by MC sampling of the full model (5000 samples), PCE of order 5 and MC sampling of the Kriging surrogate model (5000 samples). We observed excellent agreements between full model and Kriging surrogate model for both the mean values and standard deviations. The standard deviations estimated by Kriging are more accurate than PCE. The computational cost of various approaches are:

1. MC sampling of full model: 5000 samples take about 43 minutes to run.
2. PCE of order 5: re-coding efforts caused by intrusive Galerkin, plus 9 seconds to to solve for PCE coefficients.
3. Kriging surrogate model: 50 full model evaluations for the training set take about 26 seconds, plus 10 seconds to sample the Kriging surrogate models 5000 times.

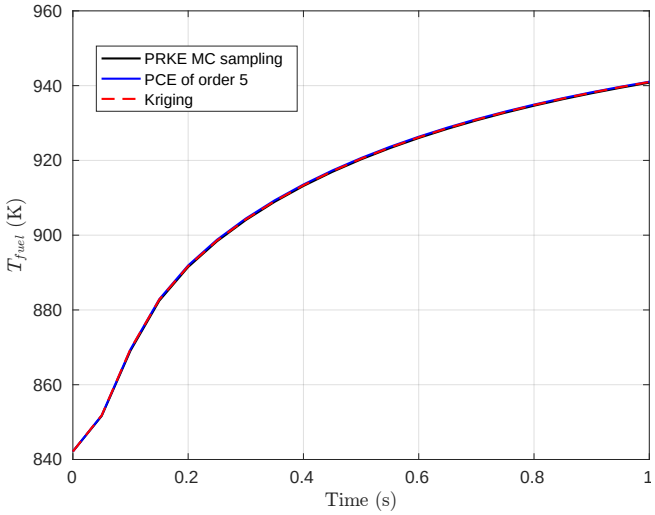

Fig. 15: Comparison of mean values of T_{fuel} computed by sampling the full PRKE model, PCE and Kriging surrogate model

We performed global sensitivity analysis [14] by calculating the Sobol' indices. Sobol' indices [15] [16] represent the part of output variance that can be attributed to each input parameter. The detailed process and results are presented in a companion paper [17]. To calculate the Sobol' indices, we used the suggested "D_3" sampling method proposed in [18]. The total computational cost of such method is $N(2d + 2)$ where d is the input dimension and N is the number of samples. Usually N is expected to be at least a few hundred to a few thousand. This is only practical by using some cheap surrogate models. Figure 17 and Figure 18 show the convergence of the main and total effect Sobol' indices for score 1 and score 2 by using different sample size N. We can see that the Sobol' indices are converging to certain equilibrium values when enough samples are used.

Figure 19 shows the converged Sobol' indices for principal component score 1 and score 2. As expected, α_c has negligible effect on both scores. ρ_{ext} accounts for over 90%

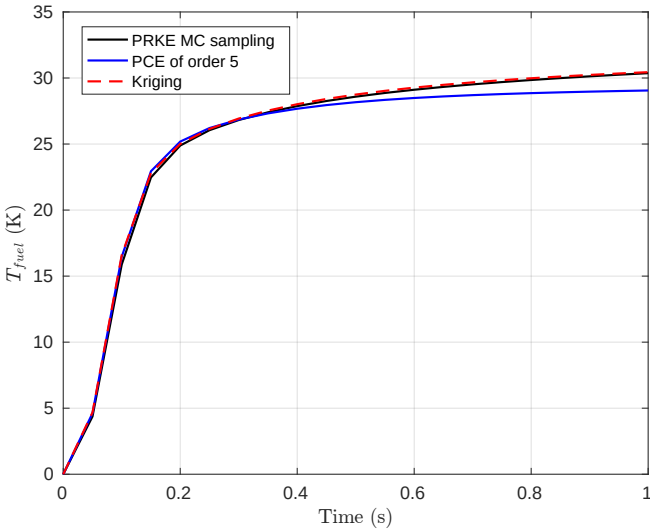

Fig. 16: Comparison of standard deviations of T_{fuel} computed by sampling the full PRKE model, PCE and Kriging surrogate model

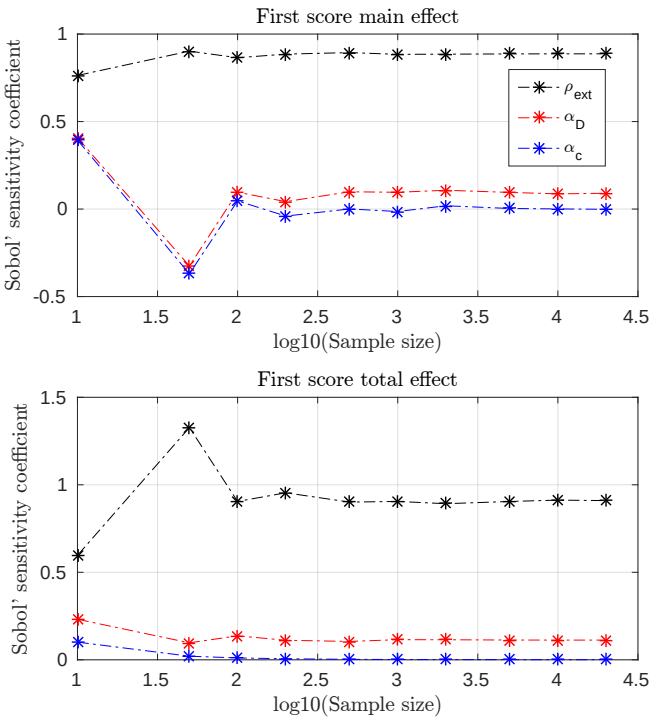

Fig. 17: Convergence of the main and total effect Sobol' indices calculated with GP surrogate model for the first principal component score

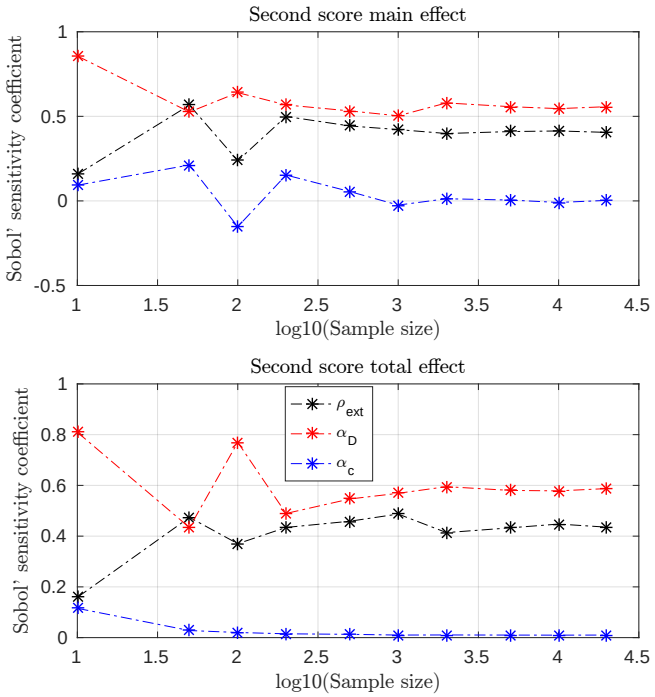

Fig. 18: Convergence of the main and total effect Sobol' indices calculated with GP surrogate model for the second principal component score

of the variation in score 1 and α_D is more important for score 2 than ρ_{ext}. Recall what we observed in Figure 9: The first principal component dominates the change of T_{fuel} with time and the second principal component represents the influence of power p on T_{fuel}. This is consistant with Sobol' indices shown in Figure 19 since ρ_{ext} changes the power directly and α_D affects the power by a negative feedback.

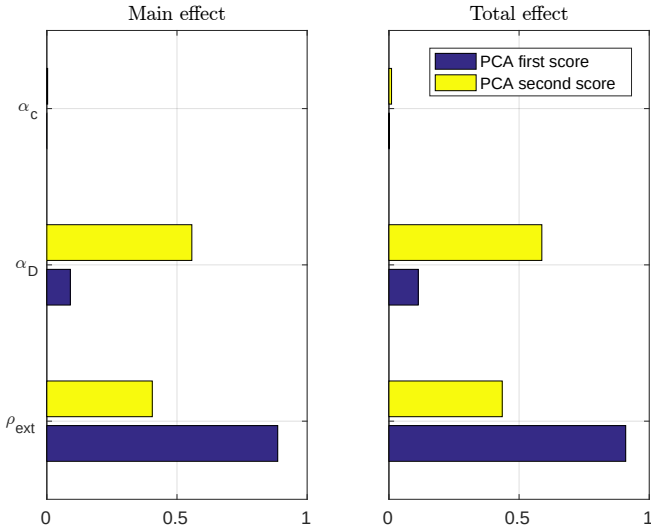

Fig. 19: Sobol' indices (main and total effects) for first and second principal component scores.

Finally, even though we have Sobol' indices available by post-processing of PCE coefficients, they are not directly comparable with the results shown in Figure 19. The Sobol' indices shown in Figure 19 are for the principal component scores, while PCE results are for T_{fuel} values. The direct comparison of Sobol' indices calculated with PCE and Kriging is presented in a companion paper [17] using a different model, in which they are shown to be very close.

V. CONCLUSIONS

In this paper, we propose to use Kriging-based surrogate models for UQ and SA in nuclear engineering. The motivation is to significantly reduce the computational cost while maintaining a desirable accuracy. It only needs the input/output relations of the full model and thus can treat the full model as a black box. Also, Kriging surrogate models can deal with higher-dimensional problem than stochastic spectral techniques like PCE.

We investigated the Point Reactor Kinetics Equation (PRKE) with lumped parameter thermal-hydraulics feedback model to compare MC sampling, PCE and Kriging surrogate model for uncertainty and sensitivity analysis. We applied PCA for the dimension reduction and it was demonstrated that the evolution of fuel temperature can be represented by only two principal components. The Kriging surrogate models are built for the principal component scores and the Kriging predictions of the scores can be mapped back to the original space, forming a time-series for the fuel temperature.

Comparison of the mean values and standard deviations of results from MC sampling of the full model, PCE and Kriging surroagte model shows that the Kriging surrogate model can accurately predict the statistical moments of the full model outputs. It only requires tens to a few hundreds of full model runs for the training and after that it can be executed in a negligible time. Kriging also has a few advantages over stochastic spectral methods like PCE: it is always non-intrusive and can deal with much higher input dimensions. Stochastic spectral methods can be non-intrusive but they always suffer from the "curse of dimensionality". To sum up, we recommend Kriging-based surrogate models for uncertainty and sensitivity analysis in nuclear engineering, especially when the compute code is very expensive.

REFERENCES

1. G. E. WILSON, "Historical insights in the development of Best Estimate Plus Uncertainty safety analysis," *Annals of Nuclear Energy*, **52**, 2–9 (2013).
2. J. D. MARTIN and T. W. SIMPSON, "Use of kriging models to approximate deterministic computer models," *AIAA Journal*, **43**, *4*, 853–863 (2005).
3. N. CRESSIE, *Statistics for spatial data*, John Wiley & Sons, revised ed. (2015).
4. M. L. STEIN, *Interpolation of spatial data: some theory for kriging*, Springer Science & Business Media (2012).
5. J. P. KLEIJNEN, "Kriging metamodeling in simulation: a review," *European Journal of Operational Research*, **192**, *3*, 707–716 (2009).
6. J. SACKS, W. J. WELCH, T. J. MITCHELL, and H. P. WYNN, "Design and analysis of computer experiments,"

Statistical Science, pp. 409–423 (1989).
7. T. J. SANTNER, B. J. WILLIAMS, and W. I. NOTZ, *The design and analysis of computer experiments*, Springer Science & Business Media (2003).
8. C. HOUSIADAS, "Lumped parameters analysis of coupled kinetics and thermal-hydraulics for small reactors," *Annals of Nuclear Energy*, **29**, *11*, 1315–1325 (2002).
9. X. WU and T. KOZLOWSKI, "Inverse uncertainty quantification of reactor simulations under the Bayesian framework using surrogate models constructed by polynomial chaos expansion," *Nuclear Engineering and Design*, **313**, 29–52 (2017).
10. X. WU, P. SABHARWALL, J. HALES, and T. KOZLOWSKI, "Neutronics and Fuel Performance Evaluation of Accident Tolerant Fuel under Normal Operation Conditions," Tech. rep., INL/EXT-14-32591, Idaho National Laboratory, Fuel Modeling and Simulation Department, Idaho Falls, Idaho (2014).
11. X. WU, T. KOZLOWSKI, and J. D. HALES, "Neutronics and fuel performance evaluation of accident tolerant FeCrAl cladding under normal operation conditions," *Annals of Nuclear Energy*, **85**, 763–775 (2015).
12. M. D. MCKAY, R. J. BECKMAN, and W. J. CONOVER, "Comparison of three methods for selecting values of input variables in the analysis of output from a computer code," *Technometrics*, **21**, *2*, 239–245 (1979).
13. A. MARREL, B. IOOSS, B. LAURENT, and O. ROUSTANT, "Calculations of sobol indices for the gaussian process metamodel," *Reliability Engineering & System Safety*, **94**, *3*, 742–751 (2009).
14. A. SALTELLI, M. RATTO, T. ANDRES, F. CAMPOLONGO, J. CARIBONI, D. GATELLI, M. SAISANA, and S. TARANTOLA, *Global sensitivity analysis: the primer*, John Wiley & Sons (2008).
15. I. M. SOBOL', "On sensitivity estimation for nonlinear mathematical models," *Matematicheskoe Modelirovanie*, **2**, *1*, 112–118 (1990).
16. I. M. SOBOL, "Global sensitivity indices for nonlinear mathematical models and their Monte Carlo estimates," *Mathematics and computers in simulation*, **55**, *1*, 271–280 (2001).
17. X. WU, C. WANG, and T. KOZLOWSKI, "Global Sensitivity Analysis of TRACE Physical Model Parameters based on BFBT benchmark," in "Proceedings of M&C-2017," Jeju, Korea, April 16-20. (2017).
18. G. GLEN and K. ISAACS, "Estimating Sobol sensitivity indices using correlations," *Environmental Modelling & Software*, **37**, 157–166 (2012).